Simulation of Circuits Demonstrating Stochastic Resonance

Gregory P. Harmer and Derek Abbott

Centre for Biomedical Engineering (CBME) and
Department of Electrical and Electronic Engineering,
University of Adelaide, 5005, South Australia

ABSTRACT

In certain dynamical systems, the addition of noise can assist the detection of a signal and not degrade it as normally expected. This is possible via a phenomenon termed stochastic resonance (SR). The response of a nonlinear system to a sub-threshold periodic input signal is optimal for some non-zero value of noise intensity. Using the signal-to-noise ratio (SNR) we can characterise SR – as the noise increases the SNR rises sharply, which is followed by a gradual decrease. We investigate the SR phenomenon in several circuits and numerical simulations. In particular, the effect that the system linearity has on the amount of gain introduced by SR and the effect of varying the input signal strength. We demonstrate, for a thresholding system, as much as a 20 dB improvement in SNR, which may be increased by further investigation.

Although SR occurs in many disciplines, the sinusoidal signal itself is not information bearing. To greatly enhance the practical applications of SR, we require operation with an aperiodic broadband signal. Hence, we introduce aperiodic stochastic resonance (ASR) where noise can enhance the response of a nonlinear system to a weak aperiodic signal. As the input signal is aperiodic, an alternate quantitative measure is required rather than the SNR used with periodic signals. We can characterise ASR by the use of cross-correlation-based measures. Using this measure, the ASR in a simple threshold system and in a FitzHugh-Nagumo neuronal model are compared using numerical simulations. Using both weak periodic and aperiodic signals we show that the response of a nonlinear system is enhanced, regardless of the signal.

Keywords: Aperiodic stochastic resonance, Noise, Nonlinear systems

1. INTRODUCTION

Noise is usually considered a nuisance in communication and signal processing systems, but via a phenomenon known as stochastic resonance (SR) noise can assist the detection of a signal. The signature of SR is recognised when the response of a nonlinear system is optimised for some non-zero value of noise. Since its emergence as a explanation for the periodic recurrences on the Earth's climate[1–4] where the term SR was first coined, SR has traversed many disciplines. These range from electronic systems,[5,6] sensing neurons,[7,8] visual perception,[9–12] bidirectional ring lasers[13] and super conducting quantum loops (SQUIDS)[14] to name a few. For further background, Gammaitoni *et al.* have written an extensive review.[15] More recently SR is believed to assist with hearing systems in the auditory nerve[16–18] while adaptive systems can learn to add the optimal amount of noise to some nonlinear feedback systems.[19]

A limitation of SR is that it only considers periodic signals, this short coming has leads to the development of a method for characterising SR with aperiodic stimuli,[20] where the term aperiodic stochastic resonance (ASR) was coined. Most of the literature regarding ASR to date has considered neuronal models.[20–27]

In this paper we first describe the types of nonlinear systems and noise that are used. This is followed by the algorithms used for numerical simulations. The next two sections replicate SR and ASR, which includes expanding ASR to the simplest nonlinear system.

2. NONLINEAR SYSTEMS & NOISE

This section describes the components that we have used to show SR and ASR. We discuss the type of noise used, followed by the nonlinear systems that we have investigated.

Correspondence: D. Abbott. (dabbott@eleceng.adelaide.edu.au).

Part of the Conference on Design, Characterization, and Packaging for MEMS and Microelectronics
Royal Pines Resort, Queensland, Australia • October 1999
SPIE Vol. 3893 • 0277-786X/99/$10.00

2.1. Noise

We used noise given by the Ornstein-Uhlenbeck (OU) stochastic process of the form

$$\dot{\zeta}(t) = \lambda\zeta(t) + \lambda\xi(t). \tag{1}$$

$\xi(t)$ is the white Gaussian noise with mean $\langle\xi(t)\rangle = 0$ and autocorrelation $\langle\xi(t)\xi(s)\rangle = 2D\delta(t-s)$, where the angled brackets $\langle\cdot\rangle$ denote an ensemble average. The correlation time of the OU process is $\tau_c = \lambda^{-1}$. The autocorrelation of the OU process is given by

$$\langle\zeta(t)\zeta(s)\rangle = \frac{D}{\tau_c}\exp(\frac{-|t-s|}{\tau_c}), \tag{2}$$

with a variance of D/τ_c. The OU process provides control over both noise intensity D, and correlation time τ_c.

2.2. Level crossing circuit

A simple level crossing detector circuit (LCC) was implemented using an operational amplifier (op amp) with the input and threshold voltage (V_{th}) applied to the non-inverting and inverting terminals respectively. The system is described by

$$v_o(t) = \begin{cases} L_+ & \text{if } v_i(t) > V_{\text{th}} \\ L_- & \text{if } v_i(t) < V_{\text{th}}, \end{cases} \tag{3}$$

where $L_\pm$ are the high and low states. In terms of circuit implementation the output is $v_o = A(v_i - V_{\text{th}})$ where A is the amplification of the op amp. When the signal exceeds the threshold voltage, the output goes high to create a variable length pulse. For all intents and purposes this suffices as an ideal LCC since the time scale of the signal is much larger than that of the op amp.

2.3. Threshold and fire

We can add some complexity to the LCC system to only output a single δ-function spike when the threshold is crossed in the positive direction. This results in a train of equal amplitude δ-spikes. The process can be described by

$$v_o(t) = \begin{cases} \delta(t-t_k) & \text{if } v_i(t) > V_{th} \\ 0 & \text{otherwise} \end{cases} = \sum_k \delta(t-t_k), \tag{4}$$

where the t_k's are the instants when the increasing output voltage crosses the threshold.

2.4. S-shaped bistable circuit

The simplest bistable nonlinear device is the comparator with hysteresis, which can be constructed using a standard Schmitt trigger.[28] This is a bistable circuit since the output voltage depends on the previous state, that is, it has memory.

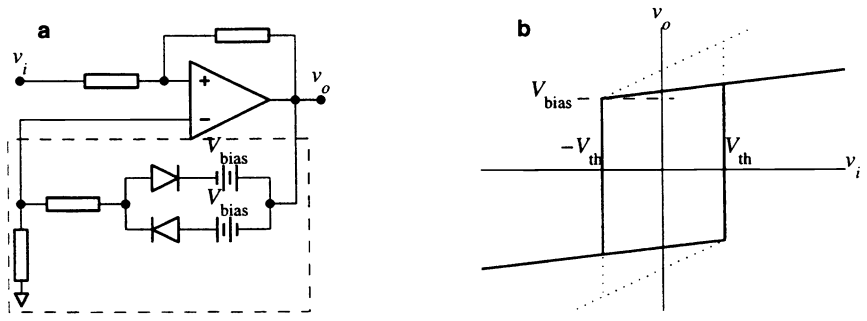

Figure 1. (a) The S-shaped operational amplifier circuit. The circuit in the dashed area are the nonlinear components that are added to the Schmitt trigger. (b) The input-output transfer characteristics of the circuit in (a).

By modifying this circuit slightly, we are able to control the positive gain of the transfer characteristic while maintaining the bistable nature. This is achieved by placing nonlinear components in the feedback path as shown in Fig. 1a, which gives the transfer characteristics in Fig. 1b. The nonlinearity of the circuit is determined by the positive gain G, it is most nonlinear for zero gain (i.e. Schmitt trigger) and becomes more linear as the gain is increased.

$$v_o(t) = \begin{cases} Gv_i(t) + C & \text{if } v_i(t) > -V_{\text{th}} \text{ and } v_o(t) \text{ high} \\ -Gv_i(t) - C & \text{if } v_i(t) < V_{\text{th}} \text{ and } v_o(t) \text{ low} \end{cases} \tag{5}$$

where $C = GV_{\text{th}} + V_{\text{bias}}$ is constant for a given G. We will refer to this type of circuit as S-shaped.

2.5. FitzHugh-Nagumo neuron model

The dynamics of the FitzHugh-Nagumo (FHN) neuronal model provide a simple representation of the firing dynamics of sensory neurons.[7,29] We consider the FHN model given by the following system that is subjected to a subthreshold signal $S(t)$, and noise given by (1)[7,30]

$$\epsilon \dot{v} = v(v-a)(1-v) - w + A + S(t) + \zeta(t), \tag{6}$$

$$\dot{w} = v - w - b, \tag{7}$$

where $v(t)$ is a fast (membrane potential voltage) variable and $w(t)$ is a slow (recovery) variable. The parameters are chosen from refs. 20 and 31, namely, $A = 0.04$, $\epsilon = 0.005$, $a = 0.5$, $b = 0.15$.

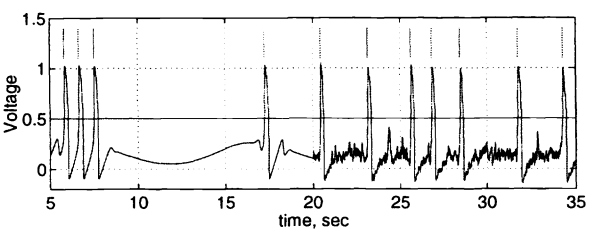

Figure 2. The first half of the FHN neuron response (fast voltage, $v(t)$) is due to a suprathreshold signal, while the right half of the response is driven by pure noise. The output is the spike train shown by the vertical lines.

The characteristics of the neuron model are shown in Fig. 2, the left half is noiseless with a suprathreshold signal while the second half is pure noise. When the sum of the time varying inputs exceeds a threshold that is determined by the FHN model, the fast membrane potential quickly increases to an excited state. Once the neuron "fires", it resets itself after a short refectory period. When this firing crosses an arbitrary threshold (set to 0.5 from refs. 7 and 31, a δ-function spike is produced. These are shown in Fig. 2 by the vertical lines above the firing periods. Hence, the output of the FHN neuronal model is a train of action potentials.

3. NUMERICAL SIMULATIONS

This section explicitly details the algorithms that were used for numerical analysis. By showing the algorithms, it should enable the reader to easily replicate the simulations.

We can approximate Gaussian white noise by choosing τ_c equal to the integration step size. The Box-Muller algorithm[32] (8-9) was used to was generate normalised Gaussian random variables from uniform random variables, and the algorithm[33] described by (10) was used to integrate the OU process to produce coloured noise. This has the advantage of allowing τ_c and the integration step size to be chosen independently while providing a noise integration accuracy of order 3/2. The algorithm is as follows, find

$$V_1 = 2\,\texttt{rand} - 1 \quad \text{and} \quad V_2 = 2\,\texttt{rand} - 1, \tag{8}$$

where rand produces a uniformly distributed random on $[0,1]$. Then calculate $S = V_1^2 + V_2^2$, which must satisfy $S < 1$, otherwise find a new V_1 and V_2. This gives the normally distributed random variables as

$$\gamma_1 = V_1\sqrt{(-2\ln S)/S} \quad \text{and} \quad \gamma_2 = V_2\sqrt{(-2\ln S)/S}. \tag{9}$$

The coloured noise is then generated by

$$\zeta_{n+1} = e^{-\alpha}\zeta_n + \sqrt{D(1-e^{-2\alpha})/\tau_c}\,\gamma_n, \tag{10}$$

where $\alpha = h/\tau_c$, and h is the integration time or step size.

Simulating the threshold systems with a stochastic process (i.e. the OU process) presents no problems, but caution must be exercised when simulating the neuron model.[34] We need to solve the deterministic ODEs of (6-7) coupled with the stochastic differential equation (SDE) of (1). The deterministic equations were numerically integrated using a fourth order Runge-Kutta (RK-4) method that is coupled with the algorithm in (8-10). In other words, solve (6-7) using the standard RK-4 algorithm, but use (10) to generate the noise for the next time step. As the RK-4 requires samples every half an integration step, a linear interpolation between the two adjacent points was used, although a simpler zero-order hold method would suffice.[35]

An aperiodic signal was constructed to demonstrate ASR according to the procedure used in refs. 21 and 31. A 10 sec unit-area Hanning window filter was convolved with coloured noise having correlation time $\tau_c = 20$ secs. The Hanning window has the affect of smoothing the signal like a low pass filter, this ensures the time scale of the signal is much greater than that of the noise.[20,27] This signal is amplified and shifted to give zero mean and variance 1.5×10^{-5}. The periodic signal consisted of a simple sinusoid with period 20 secs.

Simulations were performed with different integration and noise correlation times to determine the most appropriate choice. It was found the results did not vary significantly for step sizes less than 0.01 s, hence this is the value of h used throughout the paper. To simulate white noise, a noise correlation time equal to the integration time was used, that is $\tau_c = 0.01$ sec. It is worthy to note that when a δ-spike is produced in simulations, the discrete time version of the δ-function is used, defined as

$$\hat{\delta}(kh) = \begin{cases} 1/h & \text{if } k = 0 \\ 0 & \text{otherwise.} \end{cases} \tag{11}$$

When considering ASR, the output spike train may need to be converted to a mean firing rate, this gives an average number of spikes per second. We can achieve this by passing a 10 sec Hanning window filter over the spike train. The edge effects of the Hanning window filter were dealt with by sufficiently padding the signal with zeros.

4. REPLICATING SR

The most common way to quantify SR is through the signal-to-noise ratio (SNR),[36] which is the method used in this paper. An alternative measure for SR is via the modes of the interspike interval histograms.[10,14] The SNR is defined as the ratio of the peak signal power spectral density to the broadband background noise taken at the signal frequency and is given in decibels. The SNR is found by the equation

$$\text{SNR} = 10\log_{10}\left(\frac{S(f_0)}{B(f_0)}\right), \tag{12}$$

where S and B are the signal and background noise at the fundamental frequency f_0 respectively. The process used to calculate the SNR given the output signal from a system is shown in Fig. 3. If SR exists we expect the SNR to peak as the noise is increased, we note that this is not a *bona fide* resonant peak as the increased response is *not* due to the natural frequency of the system.[10] The alternative use of the expression 'resonance' is derived from the SNR having a peak due to some other parameter, but this definition will suffice for our purposes.

The amount of literature in SR is extensive, so we restrict ourselves to considering SR in the LCC system and the S-shaped characteristic systems. The former case will also serve as a comparison with ASR techniques while the latter investigates the role of system linearity.

Our LCC is different, although not unique,[37] from most previously studied as it produces a variable width pulse when the signal exceeds the threshold where as others produce a fixed width pulse.[38,39] The LCC circuit described

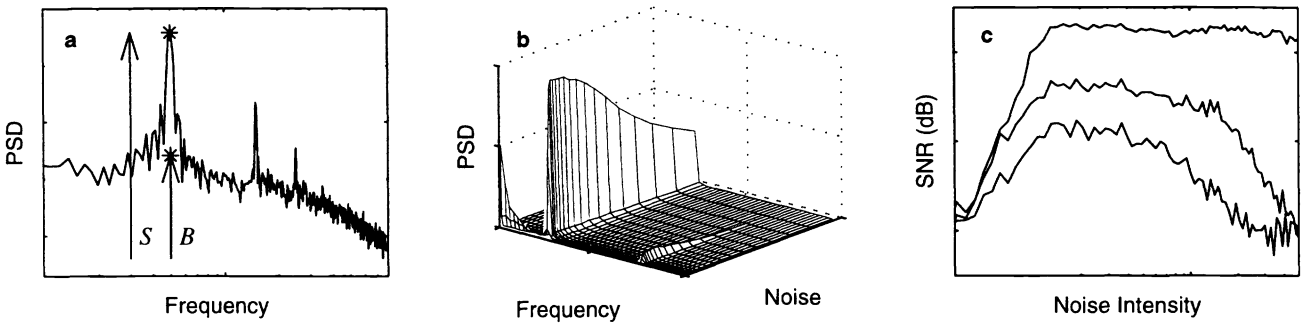

Figure 3. (a) The power spectral density (PSD) is found by taking the discrete Fourier transform of the response. (b) By taking the PSD of the response for different values of noise, a 3-dimensional plot is generated. The fundamental frequency can easily be observed. (c) The SNR for the fundamental frequency and harmonics are found from (12), as the two stars show in (a), to determine how the SNR varies with noise intensity.

in Sect. 2.2 was implemented with a threshold voltage of 0.1 V. Although the LCC is not new,[37,40] it will serve as a basis for comparison with ASR. The SNR from numerical simulations are shown in Fig. 4a. This clearly shows SR is present. The amount of improvement offered by SR is dependent on the signal-to-threshold distance, the larger the distance the smaller the improvement in SNR. Hence, when given a noisy signal one should also consider varying the threshold (if possible) as well as the noise intensity.

Several S-shaped transfer characteristics were simulated with the SNRs shown in Fig. 4b. For low noise intensities there are no transitions between the low and high states. To simplify the calculation of the SNR the dc component of the output response was removed. This helps isolate the signal component as it is not drowned out by the dc offset.

For a linear system, the response can be fully characterised in terms of linear responses theory. This means that the SNR at the output must be proportional to the SNR at the input. This is evident in Fig. 4b at low noise intensities where decreases in SNR is independent of G as the system is operating completely in the linear region. In the high noise regime, where the noise dominates the switching between states, it linearizes the system in that all the SNRs converge. The effect of the gain is most noticeable for intermediate values of noise intensity. The largest improvement in SNR is when the gain G is zero, that is, for the most nonlinear system. Similarly, when G is increased and the system becomes more linear there is less improvement in SNR. This is not totally obvious from Fig. 4b as the dc component of the response was removed.

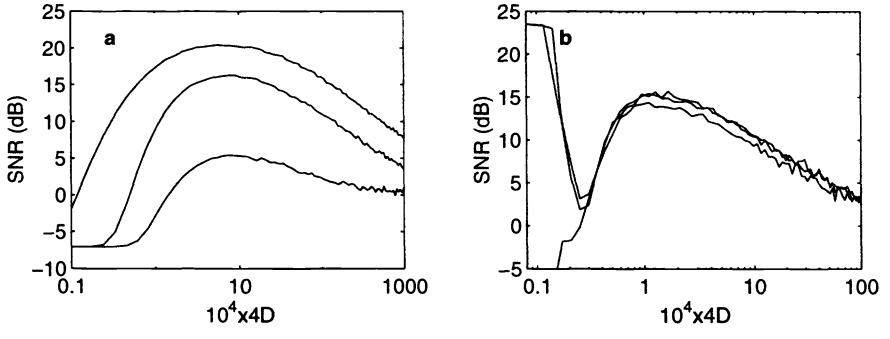

Figure 4. (a) Numerical simulations of the LCC system with a sinusoidal signal. The threshold was placed at 0.1 V and the three lines have signal amplitudes of 0.075, 0.04 and 0.01 V from top to bottom respectively. (b) Numerical simulations of the S-shaped characteristic systems. The threshold and bias were both set to 0.1 V with a signal amplitude 0.01 V. The lines have gains of 0, 2 and 10 from bottom to top.

5. REPLICATING ASR

A large proportion of work in SR has been limited to systems with periodic stimulus. Although it has served useful in many areas (Sect. 1), the applicability of SR to practical applications is limited. This is due to many real world stimuli being aperiodic.

This limitation lead to the concept of ASR, first coined by Collins *et al.*[20] ASR introduces another hindrance, namely, how to measure it. Both the methods used for SR in Sect. 4 assess the coherence of the response from the system with the input signal. These metrics are inappropriate for systems with aperiodic inputs.

A cross correlation based measure was introduced[20] that considers the correlation between the stimulus signal and the system response. This is termed the power norm C_0 and is given by

$$C_0 = \left\langle [S(t) - \overline{S(t)}][R(t) - \overline{R(t)}] \right\rangle, \tag{13}$$

where $R(t)$ is the mean firing rate signal constructed from the system output and the overbar denotes an average over time. The normalised power norm C_1 is given by

$$C_1 = \frac{C_0}{\left\langle [S(t) - \overline{S(t)}]^2 \right\rangle^{1/2} \left\langle [R(t) - \overline{R(t)}]^2 \right\rangle^{1/2}}. \tag{14}$$

These measures assume the peak in the input-output cross-correlation occur at a time lag of zero. However, in certain systems a lag may exist between the stimulus and response. In this case one should use the peak in the input-output cross-correlation function.

It has been common to use neuron models for the nonlinear system in ASR, the integrate and fire,[23,41] Hodgkin-Huxley,[23] and the FitzHugh-Nagumo[20,31,42] for example. We present our results for the FHN neuronal model in order to replicate[31] Collins *et al.* original work, which gives little detail on the numerical simulations. This is followed by the LCC system that shows ASR is possible in the simplest nonlinear system.

The FHN neuronal model described by (6-7) was used with an integration step of 0.01 sec. Fig. 5a-b shows the ensemble averaged values of C_0 and C_1 for noise intensities D over 300 trials using same aperiodic input signal.

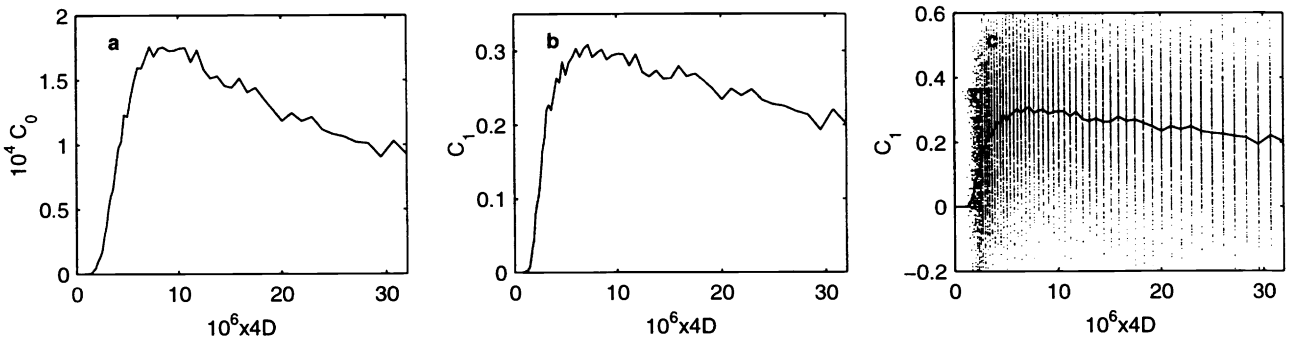

Figure 5. (a-b) The correlations C_0 and C_1 of the FHN neuronal model respectively. (c) The individual instances of C_1 showing the broad range of distributions, some even having negative correlations at the optimal noise intensity.

The results shown in Fig. 5 agree with those reported in refs. 20 and 31. Although they look promising one must take into account the distribution of the correlations.[31] In Fig. 5c, the individual trials used to generate Fig. 5b have been plotted. Even at the resonant peak, the distribution is very broad, including negative correlations between the input and output. We can gain a marked improvement by having neurons in parallel.[21,31]

Now that we have verified our ASR system we can turn our attention to the LCC system. Although a multilevel trigger system has been previously studied,[43] ASR has not been explicitly reported for the simplest implementation of a nonlinear system. The same stimulus from the FHN model was employed in the LCC with a thresholding voltage

of 0.1 V, which allows easy comparison. The results are shown in Fig. 6a-b clearly show ASR is exhibited. What this means is that using the simplest nonlinear system the input-output correlation can be improved for any signal with addition of noise. It can also be shown that ASR is also present for the simple neuron that fires whenever the threshold is crossed in the positive direction as described in Sect. 2.3.

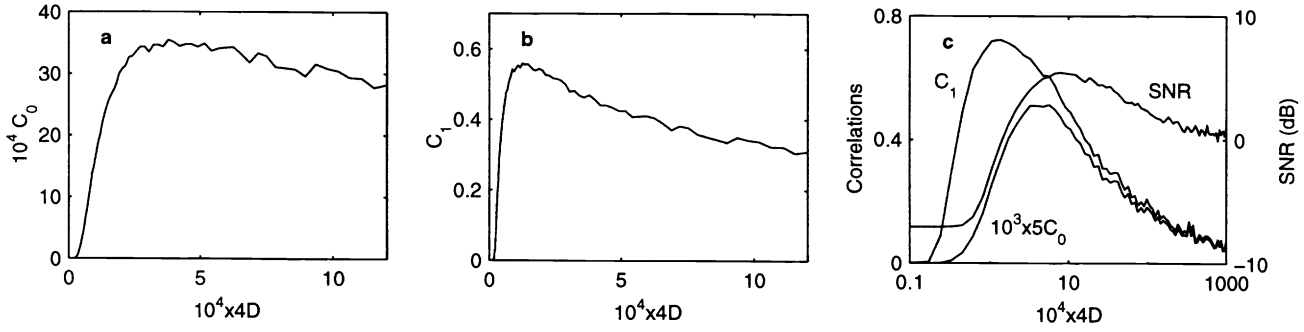

Figure 6. (a-b) Numerical simulations of the LCC system with an aperiodic signal showing the correlations C_0 and C_1. (c) A sinusoidal signal (amplitude 0.01 V) was used in the LCC system to plot both the SR metric (SNR from Fig. 4a) and the ASR metric on the same axis.

This is of interest for those who deal with simple threshold systems. One example is motion detection schemes that use insect vision models.[44] A differencing between two successive frames is needed to determine the change of intensity in each pixel. If the intensity change does not exceed a certain threshold, then no change is registered. When dealing with noisy scenes ASR may offer some assistance.

Since ASR caters for any shaped stimulus, it works equally well of a periodic signal. By using the same signal as in Sect. 4 we can compare the metrics. Fig. 6c shows SNR calculated according to (12) and the correlation coefficients calculated by (13) and (14). As we are dealing with the same signals and systems, there should not be too much discrepancy in the optimal noise value, which is supported by Fig. 6c.

6. CONCLUSION

We have explicitly provided the algorithms for the numerical simulations. This should enable the reader to easily replicate a system the exhibits ASR. Using these it was shown that ASR is present in even the simplest nonlinear system – the LCC. This exposes a wide variety of systems where ASR can be used, not just neuron models. For the first time we have explicitly demonstrated ASR in an LCC. This is of importance for motion detection models, for example, and for making a clearer performance comparison with the more widely published periodic SR results. Finally, we have seen that the two metrics for characterising the different forms of stochastic resonance are in agreement

ACKNOWLEDGMENTS

This work was funded by the Australian Research Council.

REFERENCES

1. R. Benzi, A. Sutera, and A. Vulpiani, "The mechanism of stochastic resonance," *J. Phys. A* **14**, pp. L453–457, 1981.
2. C. Nicolis, "Stochastic aspects of climate transitions response to a periodic forcing," *Tellus* **1**(34), pp. 1–9, 1982.
3. R. Benzi, G. Parisi, A. Sutera, and A. Vulpiani, "Stochastic resonance on climate change," *Tellus* **34**(1), pp. 10–16, 1982.
4. R. Monastersky, "Staggering through the ice ages: What made the planet careen between climate extremes?," *Science News* **146**, pp. 74–76, 1994.
5. S. Fauve and F. Heslot, "Stochastic resonance in a bistable system," *Phys. Lett.* **97A**, pp. 5–7, 1983.

6. V. I. Malnikov, "Schmitt trigger: A solvable model of stochastic resonance," *Phys. Rev. E* **48**(4), pp. 2481–2489, 1993.
7. A. Longtin, "Stochastic resonance in neuron models," *J. Stat. Phys.* **70**(1-2), pp. 309–327, 1993.
8. J. K. Douglas, L. Wilkens, E. Pantazelou, and F. Moss, "Noise enhancement of information transfer in crayfish mechanoreceptors by stochastic resonance," *Nature* **365**, pp. 337–339, 1993.
9. E. Simonotto, M. Riani, S. Charles, M. Roberts, J. Twitty, and F. Moss, "Visual perception of stochastic resonance," *Phys. Rev. Lett.* **78**, pp. 1186–1189, 1997.
10. L. Gammaitoni, "Stochastic resonance and the dithering effect in threshold physical systems," *Phys. Rev. E* **52**, pp. 4691–4698, 1995.
11. M. Riani and E. Simonotto, "Stochastic resonance in the perceptual interpretation of ambiguous figures: A neural network model," *Phys. Rev. Lett.* **72**, pp. 3120–3123, 1994.
12. M. Riani and E. Simonotto, "Periodic perturbation of ambiguous figure: a neural-network model and a nonsimulated experiment," *Nuovo Cimento* **17D**, pp. 903–913, 1995.
13. B. McNamara, K. Wiesenfeld, and R. Roy, "Observation of stochastic resonance in a ring laser," *Phys. Rev. Lett.* **60**, pp. 2626–2629, 1988.
14. K. Wiesenfeld and F. Moss, "Stochastic resonance and the benefits of noise: From ice ages to crayfish and SQUIDs," *Nature* **373**, pp. 33–36, 1995.
15. L. Gammaitoni, P. Hänggi, P. Jung, and F. Marchesoni, "Stochastic resonance," *Rev. Modern Phys.* **70**, pp. 223–287, 1998.
16. I. C. Bruce, M. W. White, L. S. Irlicht, S. J. O'Leary, S. Dynes, E. Javel, and G. M. Clark, "A stochastic model of the electrically stimulated auditory nerve: Single-pulse response," *IEEE Trans. Biomedical Eng.*, 1999. Preprint.
17. I. C. Bruce, L. S. Irlicht, M. W. White, S. J. O'Leary, S. Dynes, E. Javel, and G. M. Clark, "A stochastic model of the electrically stimulated auditory nerve: Pulse-train response," *IEEE Trans. Biomedical Eng.*, 1999. Preprint.
18. I. C. Bruce, M. W. White, L. S. Irlicht, S. J. O'Leary, and G. M. Clark, "The effects of stochastic neural activity in a model predicting intensity perception with cochlear implants: Low-rate stimulation," *IEEE Trans. Biomedical Eng.*, 1999. Preprint.
19. S. Mataim and B. Kosko, "Adaptive stochastic resonance," *Proc. of the IEEE* **86**(11), pp. 2152–2183, 1998.
20. J. J. Collins, C. C. Chow, and T. T. Imhoff, "Aperiodic stochastic resonance in excitable systems," *Phys. Rev. E* **52**(4), pp. 3321–3324, 1995.
21. J. J. Collins, C. C. Chow, and T. T. Imhoff, "Stochastic resonance without tuning," *Nature* **376**, pp. 236–238, 1995.
22. J. J. Collins, T. T. Imhoff, and P. Grigg, "Noise-enhanced information transmission in rat SA1 cutaneous mechanoreceptors via aperiodic stochastic resonance," *J. Neurophysiology* **76**(1), pp. 642–645, 1996.
23. J. J. Collins, C. C. Chow, A. C. Capela, and T. T. Imhoff, "Aperiodic stochastic resonance," *Phys. Rev. E* **54**(5), pp. 5575–5584, 1996.
24. J. E. Levin and J. P. Miller, "Broadband neural encoding in the cricket cercal sensory system enhanced by stochastic resonance," *Nature* **380**, pp. 165–168, 1996.
25. P. C. Gailey, A. Neiman, J. J. Collins, and F. Moss, "Stochastic resonance in ensembles on nondynamical elements: The role of internal noise," *Phys. Rev. Lett.* **79**(23), pp. 4701–4704, 1997.
26. A. Neiman, L. Schimansky-Geier, and F. Moss, "Linear response theory applied to stochastic resonance in models of ensembles of oscillators," *Phys. Rev. E* **56**(1), pp. 9–12, 1997.
27. C. Heneghan, C. C. Chow, J. J. Collins, T. T. Imhoff, S. B. Lowen, and M. C. Teich, "Information measures quantifying aperiodic stochastic resonance," *Phys. Rev. E* **54**(3), pp. 2228–2231, 1996.
28. G. P. Harmer, D. Abbott, B. R. Davis, and A. J. Parfitt, "A review of stochastic resonance: Circuits and applications," *IEEE Trans. Instrumentation and Measurement*, 1999. Submitted.
29. K. Wiesenfeld, "Stochastic resonance on a circle," *Phys. Rev. Lett.* **72**, pp. 2125–2129, 1994.
30. R. FitzHugh, "Unknown at the stage," *Biophys. J.* **1**, pp. 445–445, 1961.
31. D. R. Chialvo, A. Longtin, and J. Müller-Gerking, "Stochastic resonance in models of neuronal ensembles," *Phys. Rev. E* **55**(2), pp. 1798–1808, 1997.

32. D. E. Knuth, *The Art of Computer Programming*, vol. 2, Addison-Wesley Publishing Company, Reading, Massachusetts, second ed., 1969.
33. R. Mannella and V. Palleschi, "Fast and precise algorithm for computer simulation of stochastic differential equations," *Phys. Rev. A* **40**(6), pp. 3381–3386, 1989.
34. R. F. Fox, "Numerical simulations of stochastic differential equations," *J. Stat. Phys.* **54**(5-6), pp. 1353–1366, 1989.
35. B. R. Davis, "Numerical methods for systems excited by white noise," *Second Int. Conf. on Unsolved Problems of Noise and fluctuations*, Am. Inst. Phys., (Adelaide, Australia), 1999. In press.
36. A. R. Bulsara and L. Gammaitoni, "Tuning into noise," *Phys. Today* **49**(3), pp. 39–45, 1996.
37. F. Chapeau-Blondeau, "Noise-enhanced capacity via stochastic resonance in an asymmetric binary channel," *Phys. Rev. E* **55**, pp. 2016–2019, 1997.
38. K. Loerincz, Z. Gingl, and L. B. Kiss, "A stochastic resonator is able to greatly improve signal-to-noise ratio," *Phys. Lett. A* **224**, pp. 63–67, 1996.
39. Z. Gingl, L. B. Kiss, and F. Moss, "Non-dynamical stochastic resonance: Theory and experiments with white and arbitrarily coloured noise," *Europhys. Lett.* **29**, pp. 191–196, 1995.
40. X. Godivier and F. Chapeau-Blondeau, "Noise-assisted signal transmission in a nonlinear electronic comparator: Experiment and theory," *Signal Proc.* **56**, pp. 293–303, 1997.
41. A. R. Bulsara and A. Zador, "Threshold detection of wideband signals: A noise-induced maximum in the mutual information," *Phys. Rev. E* **54**(3), pp. 2185–2188, 1996.
42. A. Capurro, K. Pakdaman, T. Nomura, and S. Sato, "Aperiodic stochastic resonance with correlated noise," *Phys. Rev. E* **58**(4), pp. 4820–4827, 1998.
43. R. Fakir, "Nonstationary stochastic resonance," *Phys. Rev. A* **57**(6), pp. 6996–7001, 1998.
44. G. A. Horridge and P. Sobey, "An artificial seeing system copying insect vision," *Int. J. Optoelectronics* **6**(1/2), pp. 177–193, 1991.